



LIMITED DISTRIBUTION  
FOR E.E.C.

15 March, 1965

ADDENDUM TO THE PROPOSED  $K_1^0$  -  $K_2^0$  INTERFERENCE EXPERIMENT

M. Bott-Bodenhausen, X. de Bouard, D. Dekkers, B. Jordan,  
R. Mermod, P. Scharff, L. Valentin, M. Vivargent,  
T.R. Willitts and K. Winter

CERN - Institut du Radium (Orsay).

1. DETECTOR OF  $K^0$  DECAYS

The possible interference between  $K_1^0$  and  $K_2^0$  will be studied by detecting the intensity of  $K^0$  decays into two pions and into leptonic modes as a function of the distance from a regenerator inserted in a beam of  $K_2^0$ .

The detector for these decay modes should meet the following requirements:

- (i) maximum solid angle for detection of the rare  $K^0 \rightarrow 2\pi$  decay mode over one period of the beat frequency  $\Delta m$ , i.e. about  $12 \Lambda_1$  ( $\Lambda$  = mean decay length of  $K_1^0$ ).
- (ii) Electronical identification of the leptonic decays  $K_{\mu 3}^0$  and  $K_{e 3}^0$  to a level below  $K^0 \rightarrow 2\pi$  decays.
- (iii) Electronical separation of the two charged modes  $K_{\mu 3}^0 \rightarrow \pi^+ \mu^- \bar{\nu}$  and  $K_{\mu 3}^0 \rightarrow \pi^- \mu^+ \nu$  connected with the decay of  $\bar{K}^0$  and  $K^0$ , respectively, through the  $\Delta S/\Delta Q = +1$  rule.
- (iv) Suppression of the decay  $K_2^0 \rightarrow \pi^+ \pi^- \pi^0$ .
- (v) Definition of an accepted band of  $K_2^0$  momenta, above the resonance region in the channel ( $\bar{K}p$ ).

These requirements are achieved by the detector shown in Fig. 1, which is a substrate of the apparatus which proved to be successful in our first experiment<sup>1)</sup>. It makes use of the kinematical fact that in two-body decays the transverse momentum  $p_{\perp}^{K^0}$  of the secondaries is nearly constant in a wide range of c.m. angles around  $90^\circ$ . A bending magnet B gives a constant transverse momentum  $p_{\perp}^B$  in the opposite direction, such that pions emerging from a decay at  $x_{dis}$  in front of the magnet are focused in a point  $x_f$  behind the magnet :

$$x_f = \frac{x_{dis} p_{\perp}^{K^0}}{p_{\perp}^B - p_{\perp}^{K^0}}$$

Trajectories for a wide range of decay positions are defined by a coincidence of 6 scintillators. This arrangement offers two advantages:

- i) the transverse dimensions of the two beams behind the magnet are small and a threshold Cerenkov counter can be fitted in, to identify electrons,
- ii) the beams of opposite charge are well separated behind the counters  $N_4$  and  $P_4$  allowing for electronical separation of the two modes  $K^0 \rightarrow \pi^- \mu^+ \nu$  and  $\bar{K}^0 \rightarrow \pi^+ \mu^- \bar{\nu}$  by the counters  $P_5$  and  $N_5$  placed behind  $550 \text{ gr/cm}^2$  of Fe.

The solid angle for  $K^0 \rightarrow 2\pi$  decays of this detector has been calculated using Monte Carlo methods. The solid angle, averaged over a beam size of  $6 \times 15 \text{ cm}^2$ , is shown in Fig. 2 as a function of the decay position for various  $p_{K_2^0}$  momenta.

## 2. RATE OF $K_2^0 \rightarrow 2\pi$ DECAYS

The solid angles for different  $K_2^0$  momenta have to be weighted by the  $K_2^0$  momentum spectrum. We propose to derive a neutral beam at  $100 \text{ mrad}$ . The production of  $K_2^0$  at this angle is taken as the average of  $K^+$  and  $K^-$  production as observed in proton-Beryllium collisions at  $19 \text{ GeV/c}^2$ ) and shown in Fig. 3.

Using this information, the expected  $K_2^0 \rightarrow 2\pi$  distribution in time obtained from all momenta which are accepted, is shown in Fig. 4 for two different origins, at 300 and 350 cm in front of the magnet. By appropriate choice of the origin and of the absorber thickness, different parts of the interference pattern can be amplified.

The expected number of  $K_2^0 \rightarrow 2\pi$  decays per burst of  $10^{11}$  interacting protons, observed at 35 m from the target is shown in Fig. 5 as a function of the  $K_2^0$  momentum in a momentum band of 1 GeV/c. Attenuation in a 2.5 cm Pb radiator (0.9) and by decay has been taken into account. In the interval 2.5 - 6.5 GeV/c we expect to observe 0.083  $K_2^0 \rightarrow 2\pi$  decays per burst or 2500 per day.

### 3. IDENTIFICATION OF LEPTONIC DECAYS

Leptonic decays are accepted by the geometry with an average efficiency, relative to  $2\pi$  decays, of 0.2. The electrical identification of these decays was better than  $3 \cdot 10^{-3}$  in our first experiment<sup>1)</sup>. Increasing the Cerenkov angle and widening of the absorber geometry will bring this down to better than  $10^{-3}$  (for the sum of  $K_{\mu 3}$  and  $K_{e3}$ ). This leaves a background of less than  $8 \cdot 10^{-2}$  relative to  $2\pi$  decays which is to be eliminated by measurements.

Using the above-mentioned advantages of the focusing geometry, a  $K_1^0 \rightarrow K_2^0$  interference can also be detected in either charge mode of the  $K_{\mu 3}$  decays. (See paragraph 8). The transmission of pions through 550 gr/cm<sup>2</sup> Fe has been determined experimentally to be less than  $10^{-2}$  for  $p_{\pi} < 4$  GeV/c.

### 4. REJECTION OF $K^0 \rightarrow \pi^+ \pi^- \pi^0$ DECAYS

The maximum transverse momentum occurring in this decay is  $p_{\perp}^{\max} = 0.113$  GeV/c, to be compared to  $p_{\perp}^{K^0} = 0.200$  GeV/c in the decay  $K^0 \rightarrow 2\pi$ . Decays with smaller transverse momenta are accepted only over the first 100 cm of decay path, with a trigger rate of less than 0.12 relative to  $2\pi$  decays.

## 5. BACKGROUND TRIGGERS BY NEUTRON INTERACTIONS

They may occur in neutron interaction

- (i) in the regenerator which is not vetoed by the anticounter;
- (ii) in the last layer of the anticounter;
- (iii) in the mylar window of the vacuum chamber covering the decay path;
- (iv) in the first spark chamber.

These events are strongly suppressed by the trigger geometry which requires two particles of transverse momentum within a narrow band around  $p_{\perp} = 0.2$  GeV/c and of combined momentum 3 - 6 GeV/c. The integrated neutron flux above 3 GeV/c<sup>2</sup>) is  $2.6 \cdot 10^6$  neutrons/burst of  $10^{11}$  interacting protons.

The detection probability per neutron interaction has been determined with the help of the Cocconi, Koester, Perkins formula<sup>4</sup>). Its use has been justified in various production experiments. We have also compared the result of a calculation for our 10 GeV/c geometry with experimental data obtained in this geometry. According to this formula, the probability distributions in transverse and secondary momenta are independent; the probability per neutron interaction to observe a pion of given charge with  $p_{\perp}$  and  $p$  in the intervals  $dp_{\perp}$  and  $dp$  is<sup>4</sup>)

$$\frac{d^2 N}{dp_{\perp} dp} = 4 n_{\pi} \frac{p_{\perp}}{\langle p_{\perp} \rangle^2 \langle p \rangle} \exp(-p / \langle p \rangle) \exp(-2p_{\perp} / \langle p_{\perp} \rangle)$$

$n_{\pi}$  effective multiplicity of pions of given charge;

$\langle p_{\perp} \rangle$  mean transverse momentum (constant);

$\langle p \rangle$  mean secondary momentum ( $\propto p_0^{3/4}$ ).

For the 10 GeV/c geometry we obtain for the detection probability per neutron interaction

$$P_n(2\pi) = 2 \cdot 10^{-6} .$$

The following values were used for the comparison with the experimental data:

$$\begin{array}{lll} \langle p \rangle = 2 \text{ GeV/c} & \Delta p = 2.3 \text{ GeV/c} & n_{\pi} = 1 \\ p = 5 \text{ GeV/c} & p_0 = 13 \text{ GeV/c} & \\ \langle p_{\perp} \rangle = 0.3 \text{ GeV/c} & \Delta p_{\perp} = 0.02 \text{ GeV/c} & \\ p_{\perp} = 0.2 \text{ GeV/c} & \frac{\Delta \phi}{2\pi} = 0.32 & \end{array}$$

Inserting 5 gr/cm<sup>2</sup> of Carbon in the corresponding geometry, we have observed for a flux of  $5 \cdot 10^7$  neutrons/burst 7.0 triggers/burst, corresponding to

$$P_n^{\text{exp}}(2\pi) = 3.5 \cdot 10^{-6} .$$

This figure is in excellent agreement with the calculated value.

The corresponding calculation for the proposed detector was done using the following values:

$$\begin{array}{ll} \langle p \rangle = 1 \text{ GeV/c} & \Delta p = 1.5 \text{ GeV/c} \\ p = 2 \text{ GeV/c} & p_0 = 6.5 \text{ GeV/c} \\ \langle p_{\perp} \rangle = 0.3 \text{ GeV/c} & \Delta p_{\perp} = 0.06 \text{ GeV/c} \\ p_{\perp} = 0.2 \text{ GeV/c} & \frac{\Delta \phi}{2\pi} = 0.14 \\ n_{\pi} = 0.4 & \end{array}$$

with the result, obtained by integration over the intervals

$$P_n(2\pi) = 2 \cdot 10^{-5}$$

using the neutron flux for  $10^{11}$  interacting p/burst, we arrive for (iii) and (iv) at a number of false triggers

$$T_{\text{neutron}} = 3 \cdot 10^{-2} / \text{burst} .$$

The inefficient layer of the anticounter was found experimentally to be  $0.04 \text{ gr/cm}^2$ , giving rise to  $0.9 \cdot 10^{-2}$  triggers per burst. An anti-inefficiency of  $10^{-4}$  gives for  $30 \text{ gr/cm}^2$  of Carbon (i) (0.25 interaction length)  $1.3 \cdot 10^{-3}$  triggers per burst.

We expect then a total of  $0.04$  false triggers per burst, to be compared with  $0.083 \text{ K}_2^0 \rightarrow 2\pi$  triggers per burst.

All sources of false triggers are well localised and can be eliminated by rough measurements.

## 6. BACKGROUND TRACKS IN THE SPARK CHAMBERS

Neutron interactions in the regenerator will produce charged prongs which can produce accidental tracks during the sensitive time of the spark chambers.

To estimate their frequency, the Cocconi - Koester - Perkins formula has been integrated over all momenta; the angular distribution was assumed to be flat. This gives a pessimistic estimate of  $\frac{dN}{d\Omega} = 11.5$  per neutron interaction. For  $20 \text{ gr/cm}^2$  Carbon regenerator,  $10^{11}$  p interacting per burst of 300 ms and  $0.5 \mu\text{s}$  sensitive time, this gives 0.02 accidental tracks/per picture in the first and second chamber. The solid angle for the two other chambers is smaller. The analysis programme can handle one accidental track per chamber.

## 7. ANALYSIS OF PICTURES

Our flying-spot-digitizer measures at a rate of 3000 events/day. The measuring precision gives a mean error of  $\pm 0.25 \text{ mm}$  per track. All programmes for processing the data exist and are operational.

We will be able to analyse data between the runs and to change important parameters of the experiment, such as the origin and the thickness and density of the regenerator, in order to find the conditions for optimum sensitivity for the phase angle and the angular velocity  $\Delta m$  of the beat frequency.

Using the previously achieved measuring precision, we obtain the following relevant standard deviations:

$$\begin{aligned} \Delta \left( \frac{X}{\Lambda_1} \right) &= \pm 0.10 \Lambda_1 \\ \Delta M^* &= \pm 3.0 \text{ MeV} \\ \Delta \Theta &= 1 \text{ mrad.} \end{aligned}$$

### 8. PHASE OF REGENERATION AMPLITUDE

The phase as observed in the interference pattern of  $K_1^0 - K_2^0$  by the  $2\pi$  decay mode is composed of the phase  $\phi_\lambda$  between  $K_1^0$  and  $K_2^0$  and of the phase of the regeneration amplitude  $A_1$ . The latter phase,  $\phi_{A_1}$  is again composed of the phase of the scattering amplitude,  $\frac{i(\bar{f}(0) - f(0))}{2}$  and of a phase connected with the  $K_1^0 - K_2^0$  mass difference  $\Delta m$ . The phase of  $\frac{(\bar{f}(0) - f(0))}{2}$  is unknown and equal to  $\text{artg} \frac{\text{Re}(\bar{f} - f)}{\text{Im}(\bar{f} - f)}$ . In the case of  $\text{Re}(\bar{f} - f) = 0$ ,  $\Delta m = 0.7$  and thin regenerator ( $l \ll \Lambda_1$ ), this phase is  $\phi_{A_1} \cong 100^\circ$  (or  $280^\circ$  for  $\Delta m = -0.7$ ).

This phase can be determined by observation of the phase of the interference pattern in the leptonic decay mode  $K_{\mu^3}^0$ . In these decays the relative phase between  $K_1^0$  and  $K_2^0$  is known, assuming the validity of CPT and of the  $\Delta S/\Delta Q = 1$  rule :

$$\begin{aligned} \langle K_1^0 | \pi^- \mu^+ \nu \rangle &= \langle K_2^0 | \pi^- \mu^+ \nu \rangle = \frac{1}{\sqrt{2}} \langle K^0 | \pi^- \mu^+ \nu \rangle \\ \langle K_1^0 | \pi^+ \mu^- \bar{\nu} \rangle &= -\langle K_2^0 | \pi^+ \mu^- \bar{\nu} \rangle = \frac{1}{\sqrt{2}} \langle \bar{K}^0 | \pi^+ \mu^- \bar{\nu} \rangle . \end{aligned}$$

In the first case (observation of  $\pi^- \mu^+$ ) the phase equals  $\phi_{A_1}$ , in the second case (observation of  $\pi^+ \mu^-$ )  $\phi_{A_1} - \pi$ . Both cases give a pronounced interference (destructive or constructive) near to  $t = 0$ . Using the electronics identification of these decay modes, a trigger rate of

$$T_{\mu^3} = 2.4 / b$$

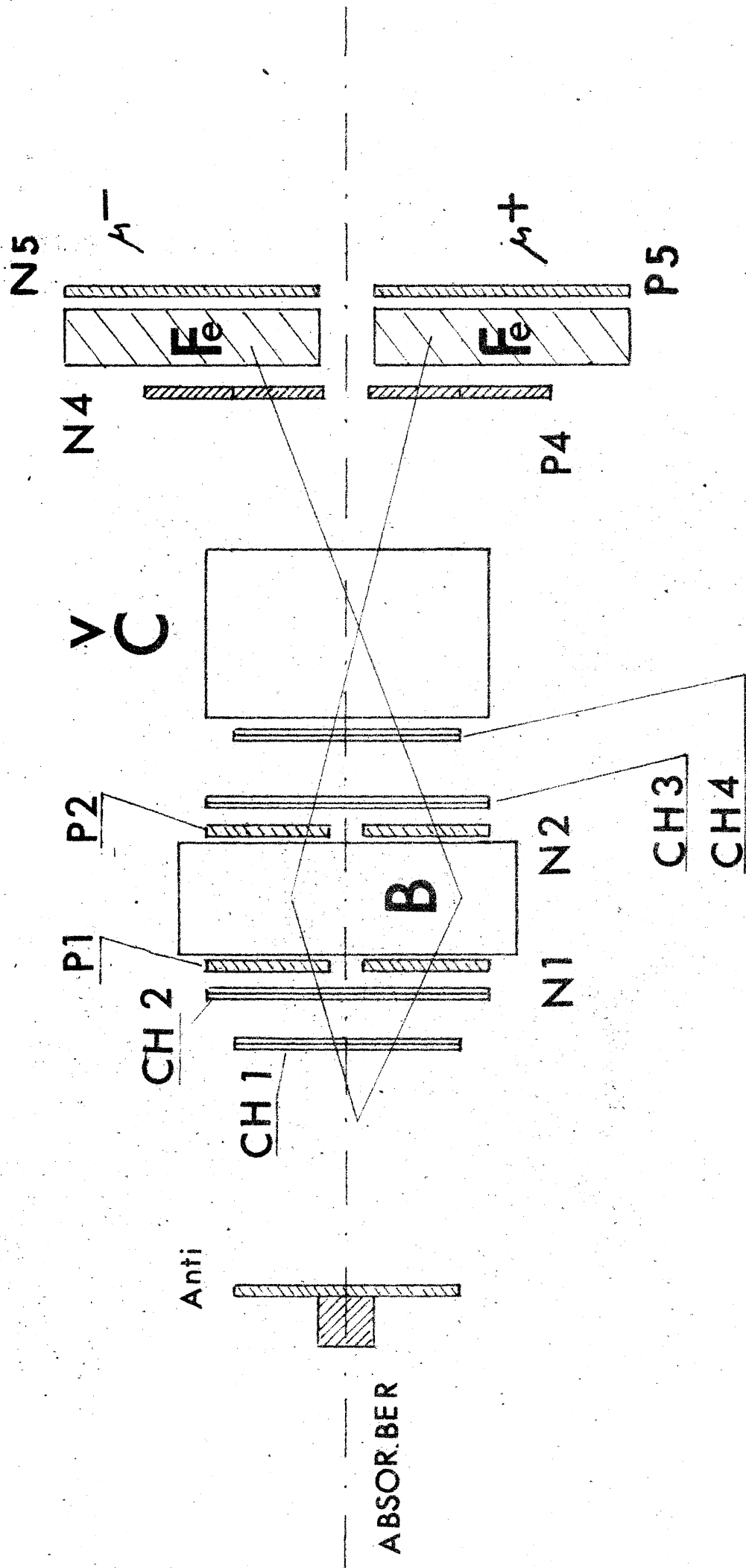
can be obtained with a contamination of  $T_{2\pi} = 8 \cdot 10^{-4} / b$  and  $T_{e^3} = 4 \cdot 10^{-3} / b$  (in the case without regenerator).

REFERENCES

- 1) X. de Bouard et al., Physics Letters 15, 58 (1965).
- 2) D. Dekkers et al., Phys.Rev. (in press).
- 3)
- 4) G. Cocconi, L.J. Koester, D.H. Perkins, UCID-1444.
- 5) K. Winter, Proceedings of 1965 Conference on Weak Interactions at Heidelberg (to be published).

\* \* \*





$K^0 \rightarrow 2\pi$  DETECTOR at  $P_{K^0} = 4 \text{ GeV} \cdot C$

Fig. 1

Acceptance (%) for  $1 K_2^0$  between 3.5 and 4.5 GeV

6.5 GeV

5.5

4.5

3.5

2.5

%

6

5

4

3

2

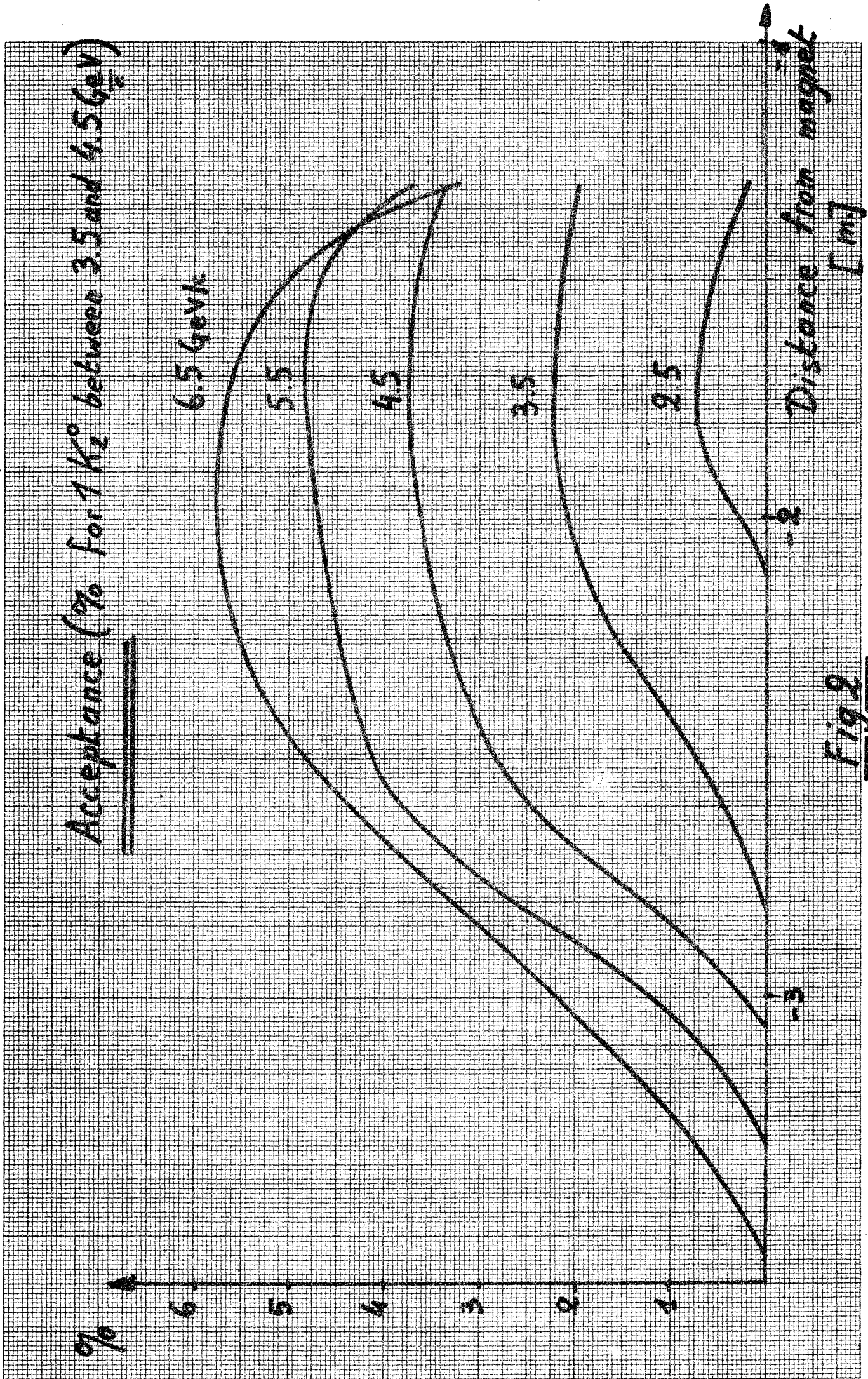
1

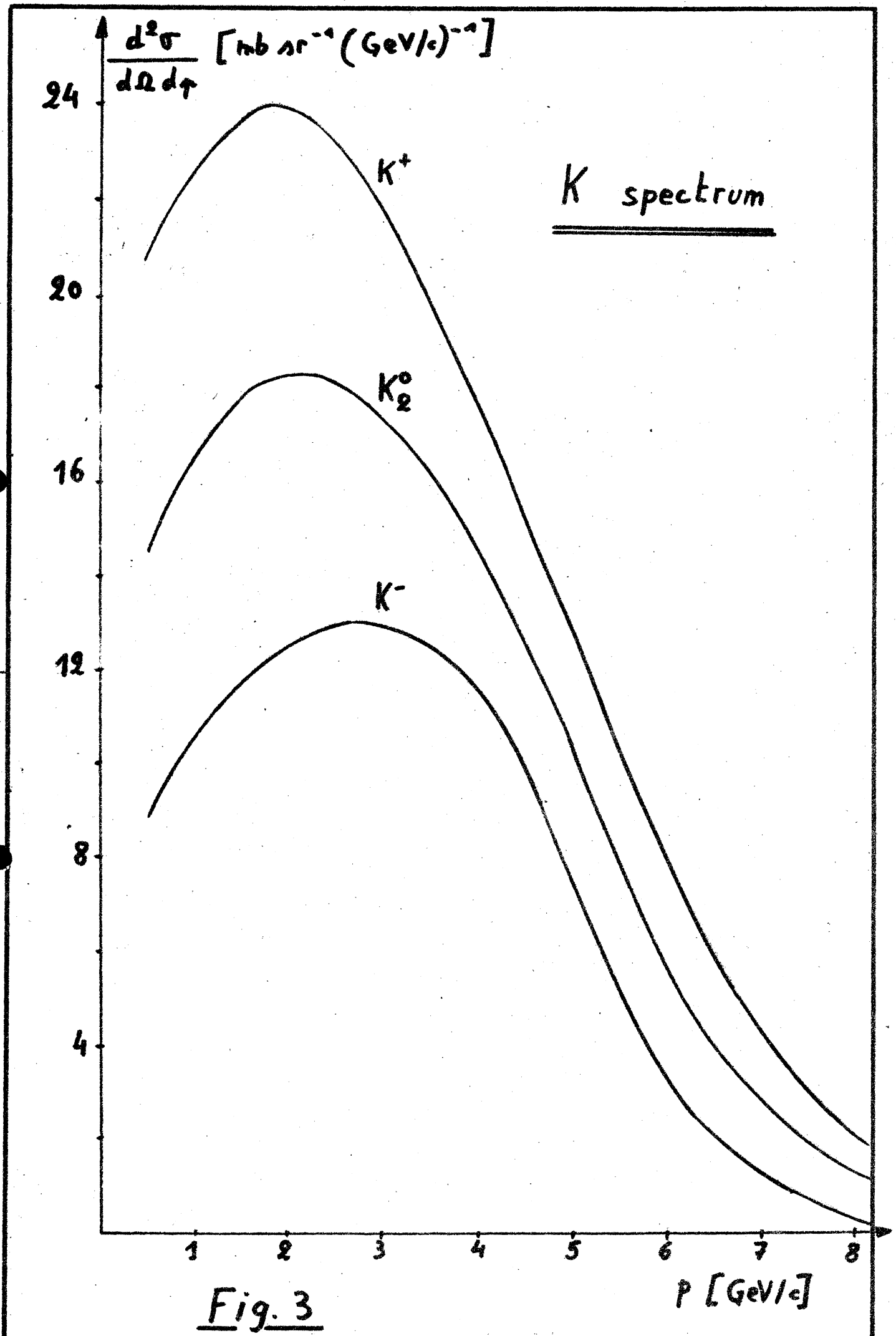
-2

-3

Distance from magnet [m]

Fig 2





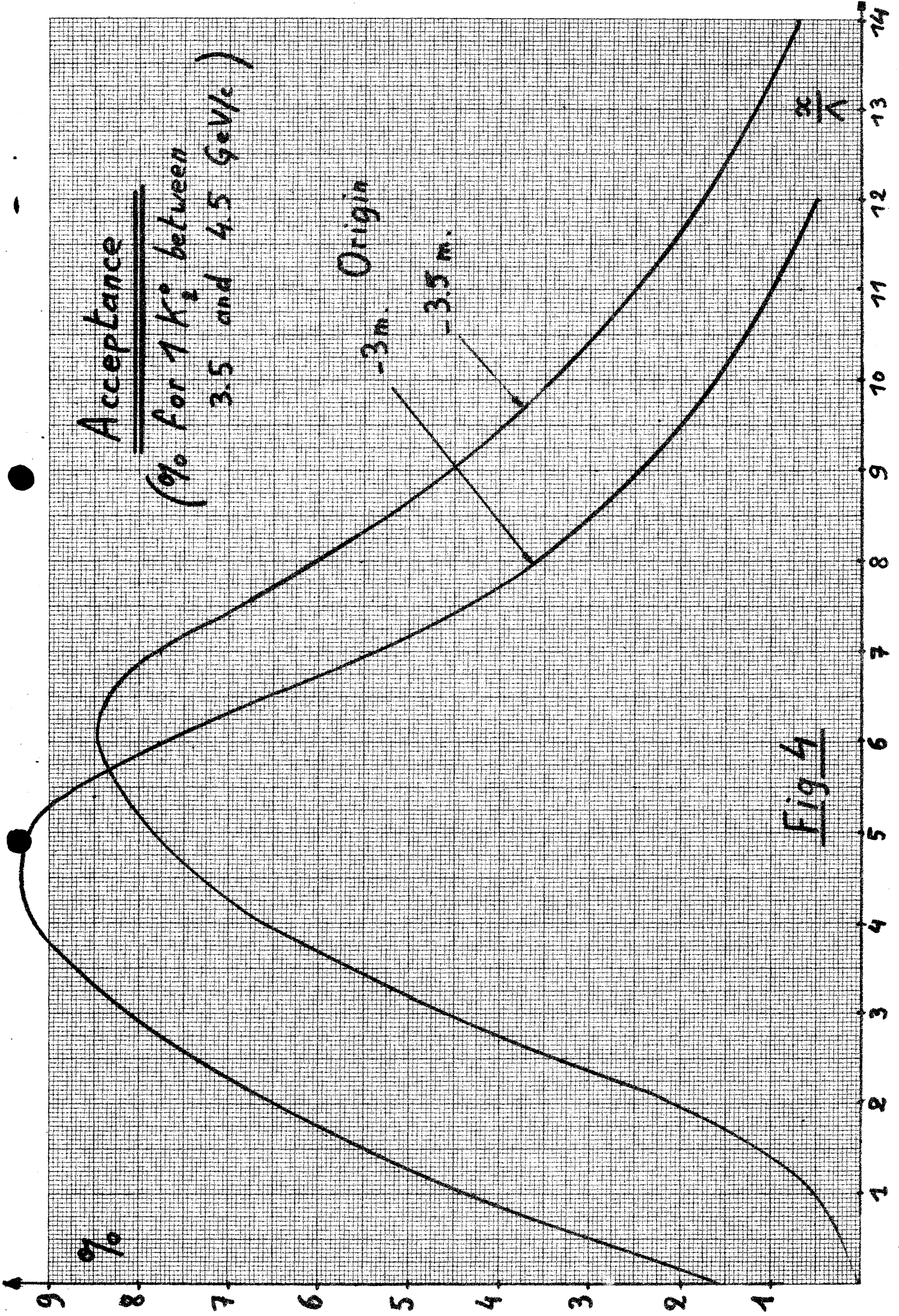


Fig 4

Trigger rate for  $K_s^0 \rightarrow 2R$  (per  $10^{10}$  protons interacting)

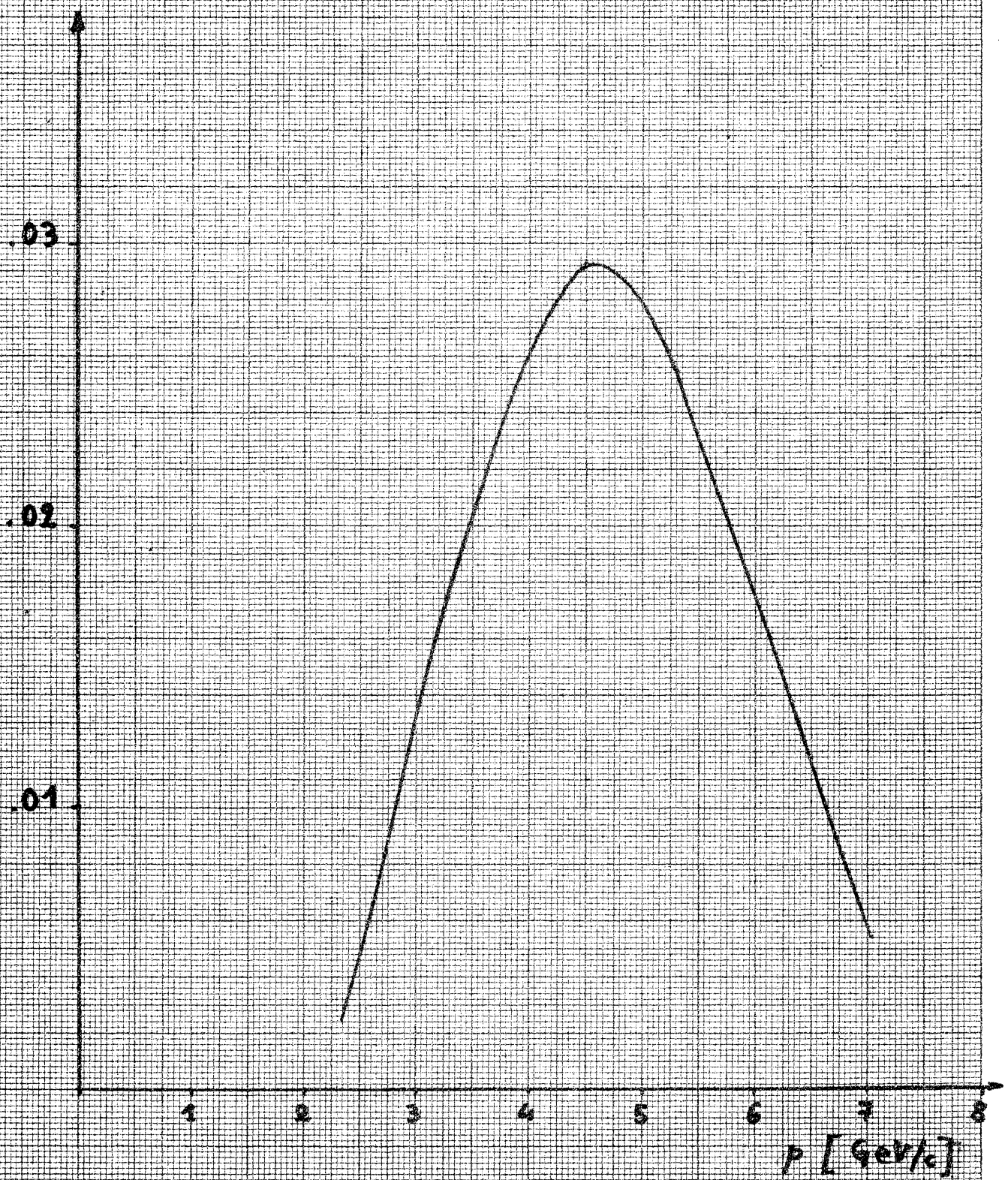


Fig. 5